International Journal of Research and Development in Applied Science and Engineering (IJRDASE)
ISSN: 2454-6844

Analyzing Lubrication of Newtonian Elastohydrodynamic Fluid in Metal-on-Metal Hip Prostheses

Shashi Kant Mishra, Nikhil Bajpai
Mechanical Engineering,
Bansal Institute of Engineering & Technology, Lucknow,
shashikantmishra151298@gmail.com, er.nikhilbajpai@gmail.com

Abstract: The research delves into several critical issues concerning the wear of artificial hip implants, with a particular focus on Metal-on-Metal (MoM) variants. It develops a simulation approach based on the Finite Element Method to study the performance of MoM artificial hip implants. The investigation involves identifying various factors responsible for wear in MoM hip implants, covering aspects such as the nonlinear behavior of lubricants, the geometry of textured surfaces, and the equations governing nominal fluid-film thickness for different types of journal bearings with non-recessed configurations. Additionally, it conducts mathematical evaluations of restrictor flow using appropriate boundary conditions.

Keywords: EHL, MOM, THR, SF

1. Introduction:

The hip joints in the human body are the spherical design type joint having the location in between the acetabulum part and the femoral head part in the pelvis wrapped by a capsule structure containing a kind of a biological lubricant known as synovial fluid (SF).This lubricant fluid works for absorbing the shocks [1]. The SF fluid with the ball and socket geometrical design type supports the hip joint design structure for transmitting the very high level of the load dynamic (6 to 8 times higher than the weight of normal human body) and associated with the a variety of critical human activity related motions. These joints are affected in aged persons suffering from chronic pain and diseases in aged people. One of the ultimate clinical solutions is the application of the total hip arthroplasty based surgery that incorporates the defected hip joint replacement from an implantation of artificial hip joint. Presently 1,00000 / 2,00000 replacements/year occurs in UK and USA and it is assumed to be increased by about 170% in the year 2030 [2,3,4]. The tribological performance are observed for the artificial joints to estimate its service life. Proper lubrication analysis helps in understanding the cause of wearing of joint surface and helps for the determination of design and manufacturing parameters.

Artificial hip joints (Fig. 1) total hip replacement (THR) design has femoral stem, sunk in the medullary canal of the femur. The alternate arrangement is resurfacing hip replacement (HRR) shown in Fig. 1. The combination of the bearing surfaces is based on the type of material, i.e. M-metal [2]. MoM implants are utilized in some selected type of patient which are younger and having extra active life style [2-4]. The wear and tear of the spherical bearing in the MoM hip joint is observed to be very highin the surface under the side loading because of the activities related to wrong positioning of joint ends.

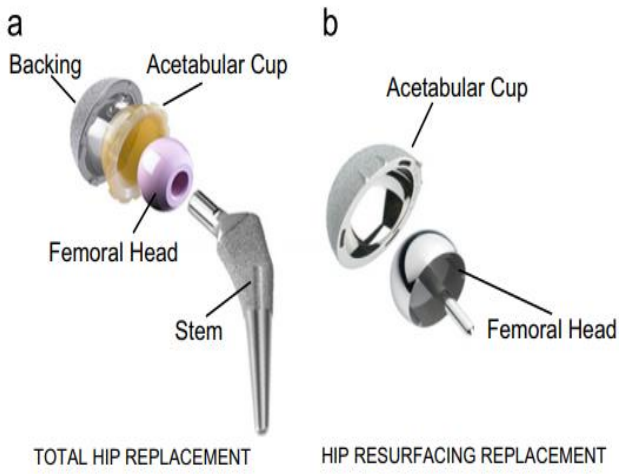

Fig. 1. Main components of an artificial hip joint.

The products generated due to metallic wearing due to friction are nanometers particles and they diffuse through the joint membranes to other body organs and causes metal toxicity [5]. It cause unfavorable reactions in the body organs with and generates the 'pseudo-tumours' [6]. In this paper elastohydrodynamic based analysis of the lubrication fluid of the MOM hip implant design is carried out. This work is very helpful for suggesting improved parameters to enhance the implantation success rate. In the paper, MOM hip joint implant elastic deformation is modeled to prediction of lubrication behavior between the surfaces. Pressure distribution fluid film at the nodal level is calculated in static and dynamic performance. The static performance includes the pressure distribution of the fluid film, maximum value of pressure, and minimum value of thickness of fluid film. The dynamic performance characteristics has considered stiffness of the lubrication fluid film and damping behavior in response of the displacement and velocity components.Artificial joint implantation is a common surgical technique. Z M Jin et al [7] analyzed lubrication and contact mechanics for hip joint that includes MoM and CoC. Gao [8] investigated MoM implant on Newton- Raphson (N-R), multi-grid (MG), multi-degree multi-integration method. Leiming [9] installed a complicated numerical version to simulate the combined lubrication based issues of a metallic-on- metallic hip prosthesis with dimpled floor texturing. In a literature [10] reviews on lubrication, stressing

based records and outcomes is performed. Similarly [11,12,13] work on cobalt-chromium (CoCr) femoral head lubricated with synovial fluid hip joints was performed. A [14,15,17] numerical simulation on wear in hip joint with a cup having a non-spherical geometry inspired by the initial stage of wear is performed. Xianjiu Lu [16,18] developed a transient visco elastic lubrication model and solved in order to investigate the influence of visco elasticity on the lubrication performance of UHMWPE artificial hip joints. Yun Peng [19] focused on quantification of the polyethylene wear on hip arthroplasty using patient-specific data through a computational model incorporating the cross-shear effect [20].

2. Related Work:

L M Gao (2006) examined elasto-hydrodynamic grease (EHL) of a metallic-on-metallic hip embed underneath semi static running conditions. Different mathematical techniques, which incorporate Newton-Raphson (N-R), multi-network (MG), multi-degree multi-mix, and quick Fourier redesign strategy (FFT), were thought of and interestingly, as far as the union and precision of the mathematical answer. It became found that the mathematical assembly for the MG approach changed into stores quicker, and thusly the computational time required changed into considerably decline than the N-R strategy. Leiming Gao,(2010) introduced a confounded mathematical model to recreate the blended EHL issue of a metal-on-steel hip prosthesis with dimpled floor finishing. The floor surface with straightforward tube shaped dimples turned out to be mathematically mimicked, underneath each steady country and going for strolls conditions.The gift outcomes showed that floor finishing may also furthermore have a surely advantageous impact on the markdown of severity contact proportion and the improvement of oil execution of metallic-on-steel hip substitutions, particularly beneath dominating limit oil conditions.

LeimingGao,(2016) presented a extensive mathematical investigation of transient non-Newtonian elastohydrodynamic grease of metal-on-metal hip prosthesis. The shear-diminishing property of the synovial liquid was found to significantly affect the greasing up film. The chief point of this examination was to investigate the job of rheology, addressed by a checked decrease of synovial liquid thickness with expanding shear rate.

QiangTian,(2017) proposed a New elastohydrodynamic (EHD) greased up round joint model for flexible multibody elements that can be utilized to display the human walk artificial hip joints. The collected conditions ofmotion for the restricted unyielding flexible multibody machine with a monstrous wide assortment of reaches offreedom are addressed utilizing the summed up alpha calculation.

Dipankar Choudhury,(2017) [70] conducted coefficient of friction (COF) checks on hip joint prostheses for fourdifferent material mixtures, without or with the presence of Ultra High Molecular Weight Polyethylene(UHMWPE) debris the use of a unique pendulum hip simulator. The results of 3 micro dimpled arrays on femoral head in opposition to a polyethylene and a metal cup had been additionally investigated. They found that clearance played a important role inthe COF of ceramic on polyethylene and ceramic on ceramic synthetic hip joints.

3. Methodology:

In this work a scheme for the computation of fluid film pressure distribution in hip implant is presented. FEM based a numerical technique is applied for getting the Reynolds equation solutions. Further, the weak formulation of the governing equation is generated for finite elements by the Galerkin's technique [21,22]. FEM based on modified Newton-Raphson method is for obtaining higher flexibility and diversity for getting the appropriate solution of partial differential equations of boundary value problems. The global system of equation governing the flow between bearings incorporates the boundary conditions i.e. equal pressure on nodes lying at holes/slots and flow of bearing being equal for the restrictor flow. The flow at hole/slot is made equal for restrictor flow equations, consequently gives the required additional equations for each hole/slot. The solution under the assumed boundary conditions gives the values of pressures at the nodal and bearing flows using FEM. The Newtonian lubricant flow exhibits non-linear behavior in terms of pressure at the node for capillary and orifice restrictor hence the Newton-Raphson as an iterative method is used to solve them. The nodal pressure distribution of fluid film is used for computing the static and dynamic behavior. The static performance described fluid film distribution, maximum pressure, and minimum thickness of the fluid film. Lubricant flow & the frictional torque evaluated under the conditions when journal is in steady state i.e. at equilibrium position. The characteristics which are observed under dynamic performance are stiffness of the fluid film and damping coefficients. These characteristics are computed by the application of pressure derivatives w.r.t. components of journal displacement and velocity respectively. Routh's criteria is finally applied to express the stability parameters of the bearing representing critical mass and stability threshold speed margin. The governing Reynolds equation to compute the flow rate between the metal and metal implant is written as [22];

$$\frac{\partial}{\partial\phi}\left(h^3\frac{\partial p}{\partial\phi}\right)+\sin(\theta)\frac{\partial}{\partial\theta}\left(h^3\sin(\theta)\frac{\partial p}{\partial\theta}\right)=6\eta R_1^2\sin(\theta)\times\left[\begin{array}{l}-\omega_x\left(\sin(\varphi)\sin(\theta)\frac{\partial h}{\partial\theta}+\cos(\varphi)\cos(\theta)\frac{\partial h}{\partial\theta}\right)\\+\omega_y\left(\sin(\phi)\sin(\theta)\frac{\partial h}{\partial\theta}-\sin(\phi)\cos(\theta)\frac{\partial h}{\partial\phi}\right)\\+\omega_z\left(\sin(\theta)\frac{\partial h}{\partial\varphi}\right)\end{array}\right]+12\eta R_1^2\sin^2(\theta)\frac{\partial h}{\partial t} \quad (1)$$

In above equation ϕ and θ are spherical coordinates $\omega_{x,y,z}$ representing the angular velocities. The Eq. 1 is expressed on non-dimensional parameter and written as

$$\frac{\partial}{\partial\phi}\left(\bar{h}^3\frac{\partial\bar{p}}{\partial\phi}\right)+\sin(\theta)\frac{\partial}{\partial\theta}\left(\bar{h}^3\sin(\theta)\frac{\partial\bar{p}}{\partial\theta}\right)=6\eta R_1^2\sin(\theta)\times\begin{bmatrix}-\bar{\omega}_x\left(\sin(\varphi)\sin(\theta)\frac{\partial\bar{h}}{\partial\theta}+\cos(\varphi)\cos(\theta)\frac{\partial\bar{h}}{\partial\theta}\right)\\+\bar{\omega}_y\left(\sin(\phi)\sin(\theta)\frac{\partial\bar{h}}{\partial\theta}-\sin(\phi)\cos(\theta)\frac{\partial\bar{h}}{\partial\varphi}\right)\\+\bar{\omega}_z\left(\sin(\theta)\frac{\partial\bar{h}}{\partial\varphi}\right)\end{bmatrix}+12\eta R_1^2\sin^2(\theta)\frac{\partial\bar{h}}{\partial t} \quad (2)$$

The following non-dimensional has been used in Eq. (2):

$$\bar{p}=\frac{p}{6\eta\omega_y(R_1/c)^2};\quad \bar{h}=\frac{h}{c} \quad (3)$$

In the above equations (1 to 3) the symbols that are used are defined below

c : Conventional clearance, (mm)

h_r : Reference fluid film thickness, (mm)

h : Local fluid-film thickness, (mm)

p : Nodal fluid film pressure, (MPa)

Q : Flow Rate, $(mm^3\cdot s^{-1})$

f_x, f_y, f_z : fluid film reactions x,y,z components

The matrices variables used are defined below:

$[\bar{F}]$: Assembled Fluidity Matrix

$\{\bar{p}\}$: Nodal Pressure vector

$\{\bar{Q}\}$: Nodal Flow vector

$\{\bar{R}_{uv}\}$: vectors representing hydrodynamic terms

$\{\bar{R}_t\}$: vector representing squeeze velocities

Reynolds equation used for lubrication analysis is non-linear hence solved by non-linear finite element method. The lubrication field pressure is :

$$p=\sum_{i=1}^{i=n}(N_i\ p_i) \quad (4)$$

On application of Galerkin's orthogonality method and element assembly scheme global system of linear equations is expressed as:

$$[\bar{\mathbf{F}}]\{\bar{\mathbf{p}}\}=\{\bar{\mathbf{Q}}\}+[\bar{\mathbf{R}}_{uv}]+\dot{\bar{h}}[\bar{\mathbf{R}}_t] \quad (5)$$

Where, an e^{th} element, the derived finite element matrix is given by.

$$\bar{F}_{ij}^e=\iint\left[\bar{h}^3\bar{F}_2\frac{\partial N_i}{\partial\phi}\frac{\partial N_j}{\partial\phi}+\bar{h}^3\bar{F}_2\left(\frac{\partial N_i}{\partial\theta}\sin(\theta)+N_i\cos(\theta)\right)\sin(\theta)\frac{\partial N_j}{\partial\theta}\right]\partial\alpha\,\partial\beta \quad (6)$$

$$\bar{Q}_i^e=\int\left[\left(\bar{h}^3\bar{F}_2\frac{\partial\bar{p}}{\partial\alpha}\right)l_1+\left(\bar{h}^3\bar{F}_2\sin^2(\theta)\frac{\partial\bar{p}}{\partial\beta}\right)l_2\right]N_i\,d\bar{\Gamma}^e \quad (7)$$

$$\bar{R}_t^e=\iint\sin^2(\theta)\,\partial\alpha\,\partial\beta \quad (8)$$

$$\bar{R}_{uv}^e=\iint h\begin{bmatrix}\sin(\theta)\begin{Bmatrix}-\bar{\omega}_x\left(\sin(\varphi)\sin(\theta)\frac{\partial N_i}{\partial\theta}+\cos(\varphi)\cos(\theta)\frac{\partial N_i}{\partial\theta}\right)\\+\bar{\omega}_y\left(\sin(\phi)\sin(\theta)\frac{\partial N_i}{\partial\theta}-\sin(\phi)\cos(\theta)\frac{\partial N_i}{\partial\phi}\right)\\+\bar{\omega}_z\left(\sin(\theta)\frac{\partial N_i}{\partial\varphi}\right)\end{Bmatrix}\end{bmatrix}\partial\alpha\,\partial\beta \quad (9)$$

The overall solution scheme using the above finite element formulation has been explained in the Fig. 2.

Following boundary condition applied for the hydrodynamic lubrication are explained below

1. Nodes lying at boundary are assigned to be zero.
2. Spherical joints Reynolds boundary conditions are:

$$\frac{\partial\bar{p}}{\partial\phi}=\frac{\partial\bar{p}}{\partial\theta}=0 \quad (10)$$

3. To describe the boundary the gauss siedle scheme is applied and the external 3D loading component is calculated as [22] ;

$$\bar{f}_x=\sum_{e=1}^{n}\bar{p}\sin^2(\theta)\cos(\phi)|J|\,d\eta\,d\zeta=-\bar{w}_x \quad (11)$$

$$\bar{f}_y=\sum_{e=1}^{n}\bar{p}\sin^2(\theta)\sin(\phi)|J|\,d\eta\,d\zeta=-\bar{w}_y \quad (12)$$

$$\bar{f}_z=\sum_{e=1}^{n}\bar{p}\sin^2(\theta)\cos(\theta)|J|\,d\eta\,d\zeta=-\bar{w}_z \quad (13)$$

Above equations is used with the convergence study. Depending on the boundary conditions and the considered geometry, however, analytical solutions is obtained. The effects of loads and boundary conditions are considered, a set of linear and nonlinear algebraic equations is considered to give the approximate behavior of the continuum or system. Pressure at a point is expressed approximately in the lubrication field. The distribution of fluid film is expressed by:

$$h = 1 - \varepsilon_x .\sin(\theta).\cos(\phi) - \varepsilon_y .\sin(\theta).\sin(\phi) - \varepsilon_z.\cos(\theta).\ \delta_r \quad (14)$$

where ε_x, ε_y, and ε_z represents the femoral head eccentric components and δ_r is the value of acetabular cup deformation in the radial direction.

4. Result and Discussion:

After getting the data matrix of nodes co-ordinates and respective elements the mesh is plotted using the input as node value, element value, element type and line style. This plot consists of a nodal mesh and an associated connectivity. X is the nodal coordinates, element is the connectivity, and element type is either 'L2', 'L3', 'T3', 'T6', 'Q4', or 'Q9' depending on the element topology.

1.	Q9	9-node quad element
2.	Q8	8-node quad element
3.	T3	3-node triangle element
4.	T6	6-node triangle element
5.	Q4	4-node quadrilateral element
6.	L2	2-node line element
7.	L3	3-node line element
8.	H4	4-node tet element
9.	B8	8-node brick element

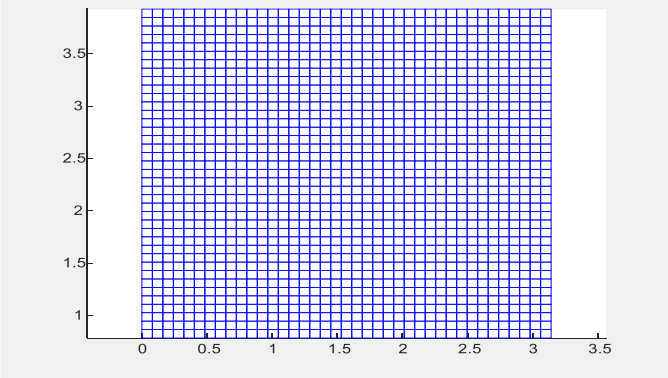

Figure 2 (a): Rectangular Mesh Region Plot for Q4 elements type representing nodal mesh and connectivity using finite number of elements to develop bearing surface.

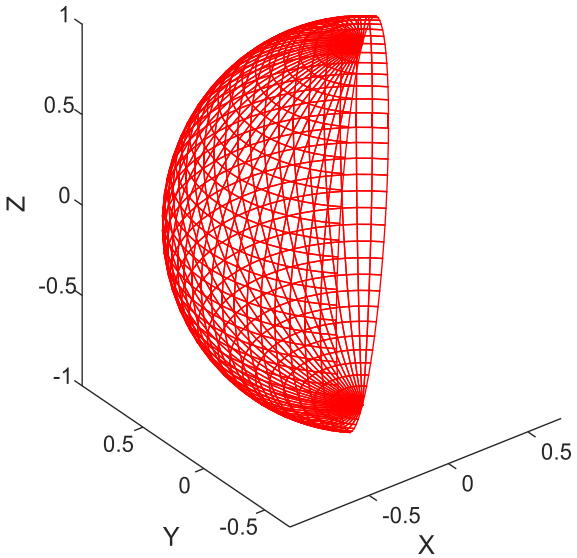

Figure 2 (b): Spherical Mesh Region Plot for Q4 elements type developed using finite element method for 3D surface generation of the spherical bearing of artificial hip implant using FEM.

After getting the rectangular mesh plot the nodes are calculated for spherical co-ordinate system to generate the spherical mesh of specified element type shown in figure 3.2 (a) and (b) for the element type choice of Q4 elements.

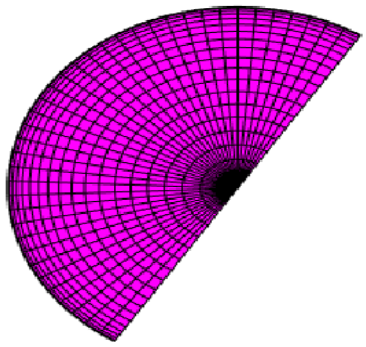

Figure 3 (a):Plot after generating 3D mesh of the spherical bearing of artificial hip implant using FEM.

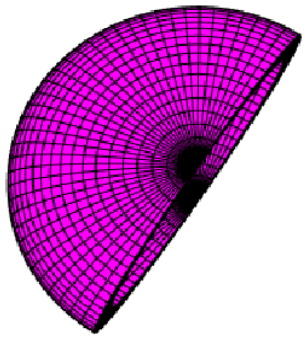

(b)

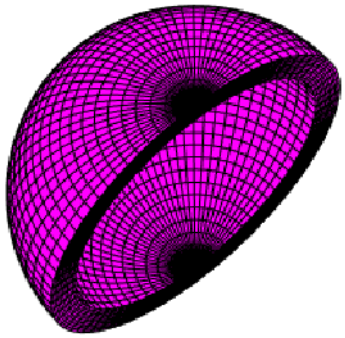

(c)

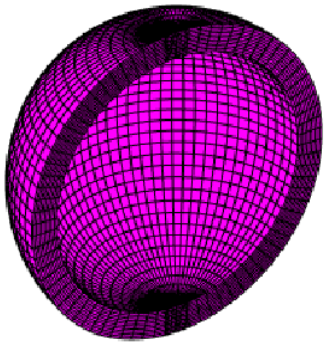

(d)

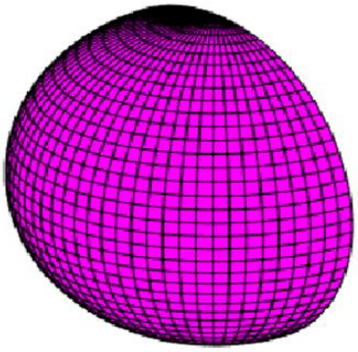

(e)

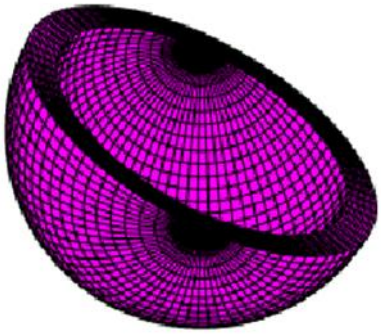

(f)

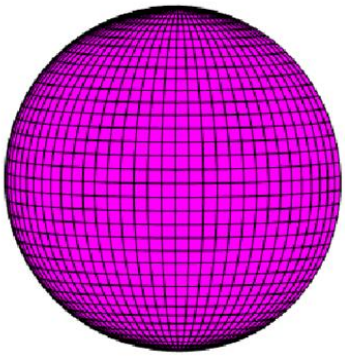

(g)

Figure 3 (b to d): Plot representing different view of 3D mesh of the spherical shaped artificial hip implant bearing structure representing inner outer surface and thickness.

3.4.4 Pressure and Stiffness Calculation:

Step 1: Initialize the variables
Step: Calculate the Gauss quadrature points
Step 3: Define Gauss quadrature order and dimension
Step 4: Apply Lagrange Basis Function for Q4 elements
Step 5: Form the Jacobian matrix
Step 6: Calculate the fluid film thickness 'h'
Step7: Determine derivative of fluid film thickness dh/dx and dh/dz
Step8: Find global shape function derivative.
Step9: Apply boundary condition
Step 10: Obtain the pressure value from Reynold equation
Step 11: Integrate the pressure value to get the fluid film reaction components
Step 12: Calculate the load carrying capacity
The function quadrature returns a n x 1 column vector W of quadrature weights and a matrix of quadrature points, where n is the number of quadrature points. After performing the above steps Gauss points are calculated the element matrix is initialized. Load, stiffness, damping and total frictional torque is calculated. Finally total load carrying capacity is evaluated to estimate the strength of joint.

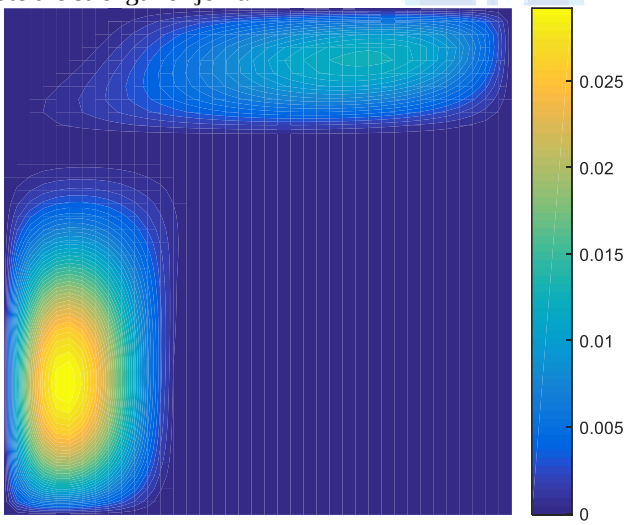

Figure 4: Contour plot for demonstrating the pressure distribution over the artificial hip joint bearing surface on application of specific load.

Pressure plot is generated and actual force and calculated force are displayed for specific boundary condition. After achieving the convergence criteria the attitude angle is defined as the angle between the line of action external load (w_o) and the line of centres of journal and bearing. The altitude angle is calculated by taking the load line and reference line for the different positions of journal centres of the attitude angle is computed. Using the stability criteria journal mass and damping

frequency is calculated to determine whether the journal design is stable or not.

5. Conclusion:

The present work consist of an approach of elastohydrodynamic lubrication analysis of MOM hip implant design by using FEM method, which has been followed up in merely few researchers in the past literature. The results which are derived in this work show that FEM technique is very useful to model the biotribological problems as compared to conventional. This approach gives faster results with better geometrical design parameters under the different types of loading condition to increase the success rate of feasibility of hip implantation. Deformation calculations are performed to get the exact prediction of fluid film distribution over the defined clearance space. This work gives the elastic deformation in the MOM implant has been model for the exact prediction of lubrication behaviour between the surface.

References:

[1] Kwon-Yong L, David P., "Compressive creep characteristics of extruded ultra high molecular weight polyethylene". J Biomed Mater Res 1997; 39:261–5.
[2] Hooke C, Huang P, "Elastohydrodynamic lubrication of soft viscoelastic materials in line contact". Proc IME J J Eng Tribol 1997;211:185–94.
[3] Jagatia M, Jalali-Vahid D, Jin ZM. "Elastohydrodynamic lubrication analysis of ultra high molecular weight polyethylene hip joint replacements under squeeze-film motion". Proc IME H J Eng Med 2001;215:141–52.
[4] Jagatia M, Jin ZM. "Elastohydrodynamic lubrication analysis of metal-on-metal hip prostheses under steady state entraining motion". Proc IME H J Eng Med 2001;215:531–41.
[5] Wang F C, Jin Z M., "Prediction of elastic deformation of acetabular cups and femoral heads for lubrication analysis of artificial hip joints". Proc IME J J Eng Tribol 2004; 218:201–9.
[6] Wang FC, Jin ZM. "Elastohydrodynamic lubrication modeling of artificial hip joints under steady-state conditions". J Tribol 2005;127:729.
[7] Z M Jin, "Analysis of fluid film lubrication in artificial hip joint replacements with surfaces of high elastic modulus," H04395 IMechE 1997 Proc Instn Mech Engrs Vol 211 Part H
[8] L M Gao, "Comparison of numerical methods for elastohydrodynamic lubrication analysis of metal-on-metal hip implants: multi-grid verses Newton–Raphson," JET228 IMechE 2007 Proc. IMechE Vol. 221 Part J: J. Engineering Tribology
[9] Leiming Gao, "Effect of surface texturing on the elastohydrodynamic lubrication analysis of metal-on-metal hip implants," Tribology International 43, 2010, 1851–1860
[10] L. Mattei, "Lubrication and wear modelling of artificial hip joints: A review" Tribology International 44, 2011, 532–549
[11] Anthony Chyr, "A patterned microtexture to reduce friction and increase longevity of prosthetic hip joints," A. Chyr et al. / Wear 315, 2014, 51–57
[12] Ehsan Askari, "Study of the friction-induced vibration and contact mechanics of artificial hip joints," Tribology International70, 2014, 1–10
[13] Leiming Gao, "A numerical study of non-Newtonian transient elasto-hydrodynamic lubrication of metal-on-metal hip prostheses," TribologyInternational93, 2016, 486–494
[14] D. Necas, "Lubrication with in hip replacements – Implication for ceramic-on-hard bearing couples," Journal of the mechanical behavior of biomedical materials 61, 2016, 371 – 383
[15] Qiang Tian, "A new elasto-hydrodynamic lubricated spherical joint model for rigid-flexible multibody dynamics," Mechanism and Machine Theory 107, 2017, 210–228
[16] Dipankar Choudhury, "The impact of surface and geometry on coefficient of friction of artificial hip Joints," Journal of the Mechanical Behavior of Biomedical Materials 72 , 2017, 192–199
[17] Leiming Gao, "Can a "pre-worn" bearing surface geometry reduce the wear of metal-onmetal hip replacements? – A numerical wear simulation study," L. Gao et al. Wear 406–407, 2018, 13–21
[18] Xianjiu Lu. "Transient viscoelastic lubrication analyses of UHMWPE hip replacements," Tribology International 128, 2018, 271–278
[19] Yun Peng, "Computational modeling of polyethylene wear in total hip arthroplasty using patient-specific kinematics-coupled finite element analysis," Tribology International 129, 2019, 162–166
[20] D. Nečas, "On the observation of lubrication mechanisms within hip joint replacements. Part I: Hard-on-soft bearing pairs," Journal of the Mechanical Behavior of Biomedical Materials 89, 2019, 237–248
[21] Yao JQ, Laurent MP, Johnson TS, Blanchard CR, Crown in shield RD. The influences of lubricant and material on polymer/ CoCr sliding friction. Wear, 2003; 255:780–4.
[22] Chaturvedi S, Bharti P K, Yadav S K, Singh S. A finite element simulation of MOM (metal-on-metal) hip implant. Lubrication Science 31(5): 210–217, 2019.